

PAPER



Cite this: *Dalton Trans.*, 2015, **44**, 1130

Interaction of a dinuclear fluorescent Cd(II) complex of calix[4]arene conjugate with phosphates and its applicability in cell imaging†‡

V. V. Sreenivasu Mummdivarapu,^a Vijaya Kumar Hinge^b and Chebrolu Pulla Rao^{*a,b}

A triazole-linked hydroxyethylimino conjugate of calix[4]arene (**L**) and its cadmium complex have been synthesized and characterized, and their structures have been established. In the complex, both the Cd²⁺ centers are bound by an N₂O₄ core, and one of it is a distorted octahedral, whereas the other is a trigonal anti-prism. The fluorescence intensity of the di-nuclear Cd(II) complex is quenched only in the presence of phosphates and not with other anions studied owing to their binding affinities and the nature of the interaction of the phosphates with Cd²⁺. These are evident even from their absorption spectra. Different phosphates exhibit changes in both their fluorescence as well as absorption spectra to varying extents, suggesting their differential interactions. Among the six phosphates, H₂PO₄⁻ has higher fluorescence quenching even at low equivalents of this ion, whereas P₂O₇⁴⁻ shows only 50% quenching even at 10 equivalents. The fluorescence quenching is considerable even at 20 ppb (0.2 μM) of H₂PO₄⁻, whereas all other phosphates require a concentration of 50–580 ppb to exhibit the same effect on fluorescence spectra. Thus, the interaction of H₂PO₄⁻ is more effective by ~30 fold as compared to that of P₂O₇⁴⁻. Fluorescence quenching by phosphate is due to the release of **L** from its original cadmium complex via the formation of a ternary species followed by the capture of Cd²⁺ by the phosphate, as delineated based on the combination of spectral techniques, such as absorption, emission, ¹H NMR and ESI MS. The relative interactive abilities of the six phosphates differ from each other. The removal of Cd²⁺ is demonstrated to be reversible by the repeated addition of the phosphate followed by Cd²⁺. The characteristics of the ternary species formed in each of these six phosphates have been computationally modeled using molecular mechanics. The computational study revealed that the coordination between cadmium and –CH₂–CH₂–OH breaks and new coordination is established through the phosphate oxygens, and as a result the Cd²⁺ center acquires a distorted octahedral geometry. The utility of the complex was demonstrated in HeLa cells.

Received 10th June 2014,
Accepted 4th November 2014

DOI: 10.1039/c4dt01726a

www.rsc.org/dalton

Introduction

In living systems, phosphates are found as inorganic phosphates (Pi) and pyrophosphates (PPi), and also as biologically active molecules, such as adenosine mono-, di- and tri-phosphates (AMP, ADP and ATP), and ribo- and deoxyribo-nucleic

acids (RNA and DNA), to mediate several essential biological functions.^{1,2} Creatine phosphate (CP) is a phosphorylated creatine that serves as intracellular energy shuttle, which facilitates the transport of ATP from muscle cell mitochondria to myofibrils.^{2e} The excess of phosphate results in kidney failure, while its deficiency leads to hyperthyroidism.³ However, in ecological systems, these are mainly found either in the form of calcium hydroxyapatite or as salts of heavy metal ions, such as Cd²⁺, Pb²⁺, Cu²⁺ and U^{4+/5+}.⁴ Among these cations, concentrations of relatively toxic Cd²⁺ is significantly affected by the phosphate contents present in its particular environmental condition.⁵ The quantification of such interrelated ions and species using synthetic molecular receptors is very important in deriving conclusions about certain diseases or environmentally related issues, including disease diagnosis.⁶ Recently, calix[4]arene scaffolds have been used as a platform to build receptors for recognizing and sensing ions and molecules by eliciting appropriate fluorescence, absorbance and/or color

^aDepartment of Chemistry, Indian Institute of Technology Bombay, Powai, Mumbai 400 076, India

^bDepartment of Biosciences & Bioengineering, Indian Institute of Technology Bombay, Powai, Mumbai 400 076, India. E-mail: cprao@iitb.ac.in; Fax: +91 22 2572 3480; Tel: +91 22 2576 7162

†This paper has been dedicated to Professor C.N.R. Rao, FRS on his 80th birthday.

‡Electronic supplementary information (ESI) available: ¹H and ¹³C NMR, mass spectral data of **L** and [CdL]₂, fluorescence and absorbance spectra of all the anions, ¹H NMR titration of [CdL]₂ with phosphates, crystal data for [CdL]₂, and the computational data. CCDC 1007749–1031377. For ESI and crystallographic data in CIF or other electronic format see DOI: 10.1039/c4dt01726a

signals.^{7–9} In the past few years, a class of pillararenes has significantly emerged, which are used as new receptor systems for recognizing ions and molecules.¹⁰ Cd^{2+} is known to induce fluorescence enhancement upon binding to non-fluorescent molecules.¹¹ The metal ion-bound fluorescent molecular species can act as secondary sensors for specific anions and/or amino acids, although their modes of interaction are poorly understood.¹² Therefore, the present manuscript accounts for a detailed interaction aspects of phosphates and nucleotides using a crystallographically characterized di- Cd^{2+} complex of newly synthesized triazole-linked calix[4]arene possessing $-\text{N}-\text{CH}_2-\text{CH}_2-\text{OH}$ terminal moiety on an imino-phenolic core, *viz.*, $[\text{CdL}]_2$ using experimental and computational studies.

Results and discussion

Receptor molecule **L** has been synthesized by the condensation of **P** with ethanolamine as shown in Scheme 1. The triazole-linked hydroxyethylimino conjugate of calix[4]arene (**L**) possessing an imino-phenolic core has been synthesized by adopting the procedures similar to those previously developed by us, and was confirmed through characterization as given in the Experimental section (ESI,† SI01).¹³

Synthesis and characterization of the cadmium complex

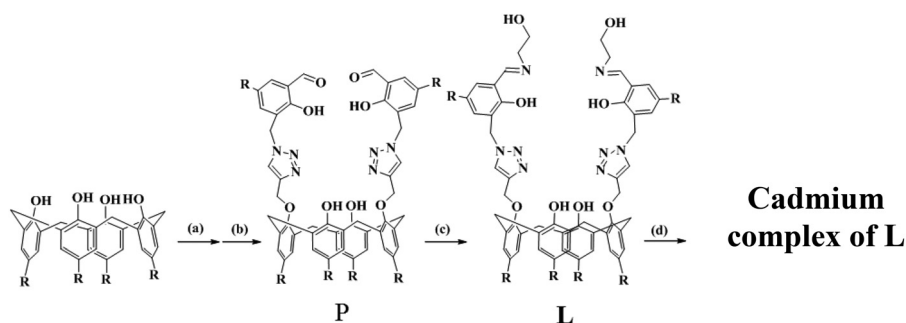
The Cd^{2+} complex of **L** has been synthesised by reacting **L** with cadmium acetate in methanol followed by refluxing the reaction mixture for 12 h, as shown in Scheme 1, and the details are given in the Experimental section (ESI,† SI02). The resultant complex was isolated as a solid product and was well characterized by ^1H and ^{13}C NMR, ESI MS and elemental analysis.

^1H NMR spectrum of **L** and its cadmium complex in $\text{DMSO}-d_6$ were compared to determine the complex formation (Fig. 1a, b). Upon complexation, the imine- and $-\text{CH}_2-\text{CH}_2-\text{OH}$ protons show downfield shifts of about 0.2 and 0.75 ppm, respectively, whereas the triazole and aromatic protons experience upfield shifts of 0.10 and 0.35 ppm, respectively, suggesting the binding of Cd^{2+} with the imino-phenolic core, including the terminal $-\text{CH}_2-\text{CH}_2-\text{OH}$ moiety. ^1H NMR spectrum of $[\text{CdL}]_2$ supported the presence of cone conformation,

as can be noticed from the appearance of peaks at 3.06 and 3.90 ppm for the $-\text{CH}_2$ bridge moiety, and correlation between these two protons, *viz.*, m' and n' , can be observed (Fig. 1c, d). In two-dimensional spectroscopy, the correlation between $-\text{CH}_2-\text{CH}_2-\text{OH}$ and $-\text{OCH}_2$ was observed from the cross peak obtained between j' and l' , supporting the involvement of $-\text{CH}_2\text{OH}$ in the complex (Fig. 1e). The cone conformation is intact even when the complex is formed, as the cross peak between m' and n' is retained. The involvement of $-\text{C}=\text{N}-$ in binding to Cd^{2+} has also been assumed from the shift observed in the stretching vibration from 1638 to 1645 cm^{-1} upon complex formation (Fig. 1f, g). The $m/z = 2776.41$ peak observed in the ESI mass spectrum corresponds to the formation of the cadmium complex as 2 : 2, *viz.*, $[\text{CdL}]_2$, and the presence of Cd^{2+} was unambiguously confirmed from the observed isotopic peak pattern, which agrees well with the calculated one (Fig. 1h, i).

Structural aspects of the cadmium complex

Single crystals of the cadmium complex were generated by slow evaporation of a solution of this product that was dissolved in $\text{DMSO}:\text{CHCl}_3$ taken in 1 : 3 v/v ratio. The details of the data collection and the structural refinement are presented in the Experimental section (ESI,† SI03). Each calix[4]arene unit found in the complex exhibits two intramolecular $\text{O}-\text{H}\cdots\text{O}$ hydrogen bonds at the lower rim, and as a result of this the calix[4]arene adopts a cone conformation. These hydrogen bonds, *viz.*, $\text{O00A}-\text{H}\cdots\text{O009}$ (1.99 Å, 2.79 Å and 156.3°), $\text{O006}-\text{H}\cdots\text{O007}$ (2.04 Å, 2.87 Å and 165.7°), are responsible for maintaining the cone conformation. This has been a common phenomenon and is observed in almost all the 1,3-di-conjugates of calix[4]arene that form cone conformation.¹⁴ The cone conformation of the calix[4]arene moiety was also confirmed by ^1H NMR spectroscopy. The dinuclear nature of the complex was supported by the ESI† peak observed at $m/z = 2776.41$ (Fig. 1h). Because the overall dinuclear complex is neutral, each calix[4]arene conjugate acts as dianionic species, which is formed by the deprotonation of both the phenolic-OH groups present on the arms (Fig. 2). The cadmium centers present in the dinuclear complex are bound by a N_2O_4 coordination core, and this part is connected between one arm of each calix[4]arene,



Scheme 1 Synthesis of the cadmium complex of calix[4]arene conjugate, $[\text{CdL}]_2$. (a) K_2CO_3 , propargyl bromide, dry acetone, 16 h; (b) 5-*tert*-butyl-3-(azidomethyl)-2-hydroxybenzaldehyde, $\text{CuSO}_4\cdot 5\text{H}_2\text{O}$, sodium ascorbate, $\{\text{CH}_2\text{Cl}_2:\text{tert}-\text{BuOH} (1:1):\text{H}_2\text{O} (1:1)\}$, 24 h; (c) ethanol amine, CH_3OH , 12 h; (d) $\text{Cd}(\text{CH}_3\text{COO})_2\cdot 2\text{H}_2\text{O}$, CH_3OH , 12 h, reflux. R = *tert*-butyl.

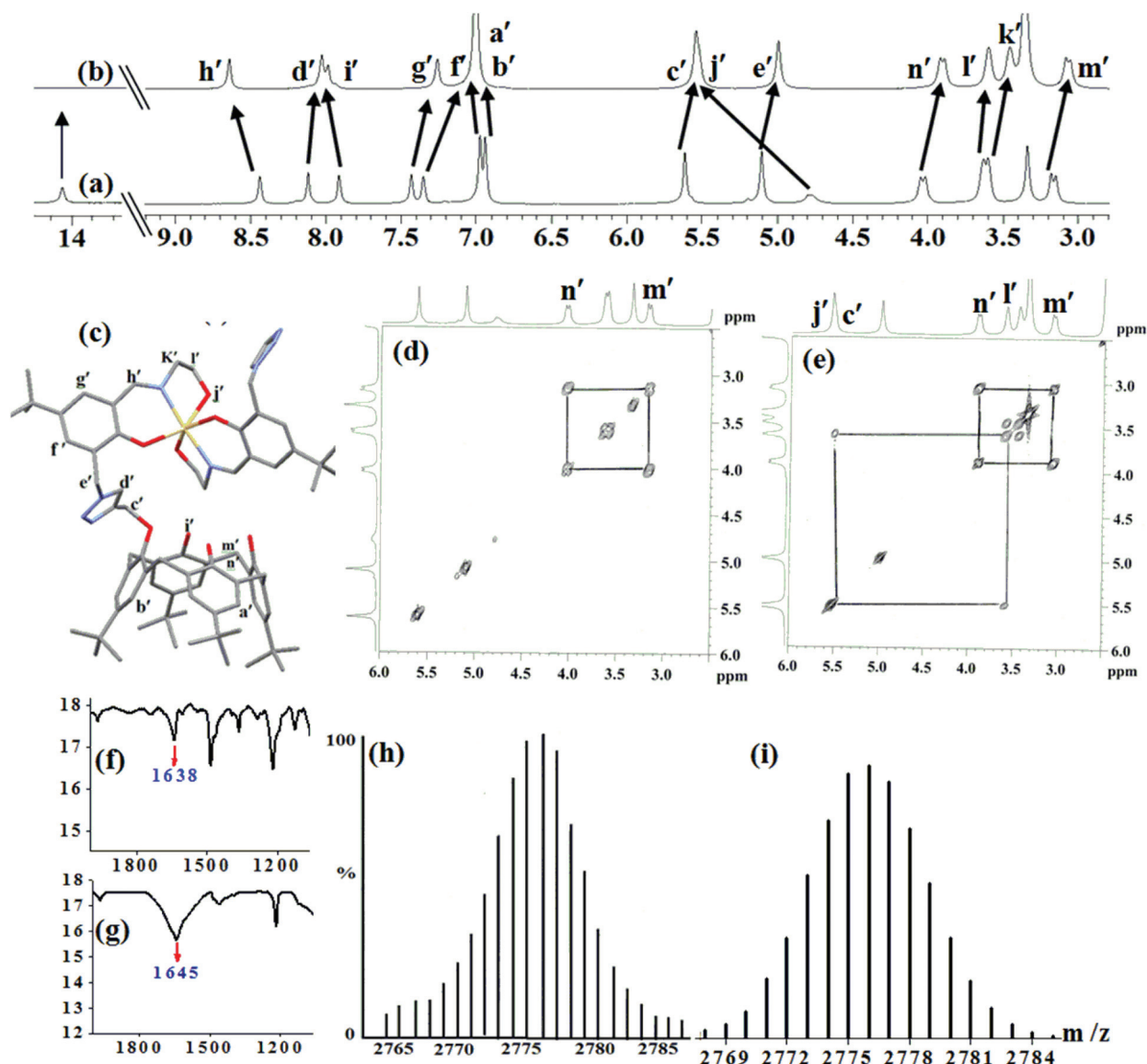


Fig. 1 ¹H NMR spectra: (a) L, (b) [CdL]₂. (c) Proton labeled structure. 2D COSY spectra: (d) L, (e) [CdL]₂. FTIR spectra: (f) L and (g) [CdL]₂. Mass spectral isotopic peak pattern of cadmium in [CdL]₂: (h) experimental and (i) calculated. NMR solvent used in these studies was DMSO-d₆.

where each arm supports NO₂ coordination. Thus, the overall geometry about Cd1 cadmium is distorted octahedral, whereas Cd2 is distorted trigonal antiprismatic, and the coordination core around each Cd²⁺ comprises of two phenolic oxygens, two imine nitrogens and two ethanolic hydroxyl groups. The Cd1–O bond length is longer by 0.17 Å in the case of –CH₂–CH₂–OH that bound as neutral –OH as compared to the phenolic oxygen due to its deprotonation. This is further elongated in case of Cd2.

Interaction of phosphates with cadmium complex

The calix[4]arene receptor L, exhibits low fluorescence owing to the isomerization of the imine (C=N bond) and also due to the excited-state intramolecular proton transfer (ESIPT) from salicyl –OH to the imine nitrogen in the excited state.¹⁵ The binding of Cd²⁺ to L prevents the isomerization as well as

ESIPT, thus exhibiting a fluorescence enhancement by its complex. In addition, a chelation-enhanced fluorescence (CHEF)¹⁶ also contributes to the fluorescence of the complex. Thus, the Cd²⁺ is responsible for fluorescence enhancement because simple L alone is weakly fluorescent. Therefore, the cadmium complex has been used for the study of the interaction of anions, in particular, the phosphates. In the case of interaction by an anion, the complex is expected to exhibit spectral changes amounting to its nature and extent of binding. Thus, the study of the interaction of anions has been addressed by emission, absorption, ESI MS and ¹H NMR studies.

Fluorescence spectra

The interaction of the cadmium complex with several anions, including phosphates, *viz.*, F[–], Cl[–], Br[–], I[–], ClO₄[–], N₃[–],

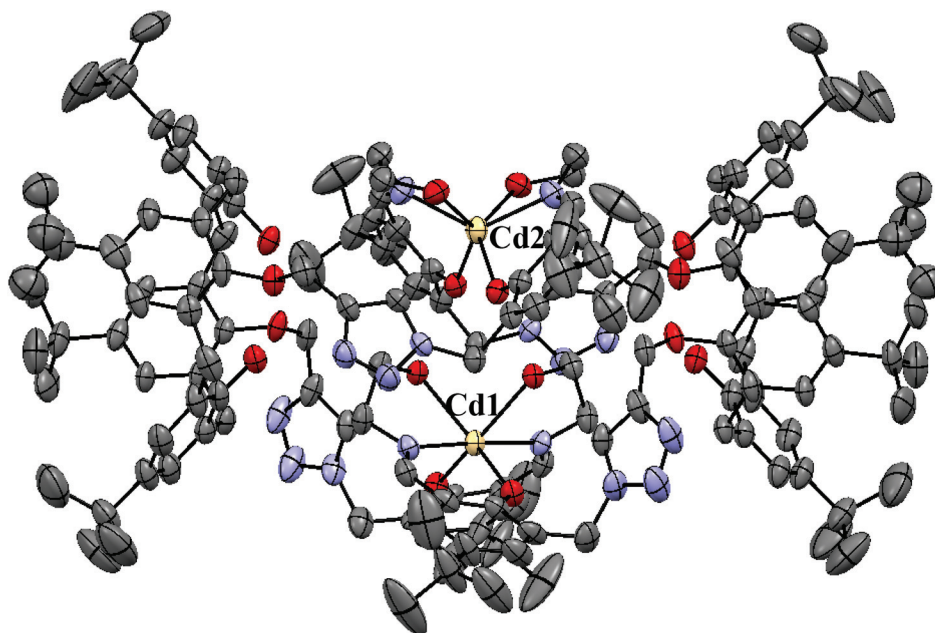


Fig. 2 Crystal structure of the cadmium di-nuclear complex.

CH_3COO^- , SCN^- , CO_3^{2-} , HCO_3^- , NO_2^- , NO_3^- , HSO_4^- , SO_4^{2-} , H_2PO_4^- , HPO_4^{2-} and $\text{P}_2\text{O}_7^{4-}$ (PPI), has been examined by carrying out fluorescence spectral studies in ethanol. These studies could not be carried out in buffer solutions as the fluorescence of the complex is quenched even in the absence of the anion (ESI,† SI 04). All the anions, except phosphates, show no changes in the fluorescence of the cadmium complex. In case of H_2PO_4^- , it exhibits a complete quenching at ~ 4 equivalents, whereas all the other five phosphates show considerably less quenching than that of H_2PO_4^- . Thus, only the phosphate-based anions exhibited fluorescence quenching of the complex to different extents (Fig. 3b and ESI,† S05–S06). Four equivalents of phosphate addition results in complete quenching ($98 \pm 2\%$) in the case of H_2PO_4^- , but only $83 \pm 2\%$ in the case of HPO_4^{2-} , ADP^{2-} and ATP^{2-} , $70 \pm 2\%$ in the case of AMP^{2-} , and it is $31 \pm 2\%$ in the case of $\text{P}_2\text{O}_7^{4-}$. Even at 10 equivalents of phosphate addition, the fluorescence quenching is incomplete in the case of AMP^{2-} and $\text{P}_2\text{O}_7^{4-}$, and it is $85 \pm 2\%$ and $51 \pm 2\%$, respectively (Fig. 3a). Thus, a 50% fluorescence quenching is achieved only with 2 to 2.5 equivalents of H_2PO_4^- ; however, the same is achieved at ~ 10 equivalents in the case of $\text{P}_2\text{O}_7^{4-}$. Among the biologically relevant nucleotides studied, the fluorescence quenching of the complex follows a trend, $\text{ATP}^{2-} > \text{ADP}^{2-} > \text{AMP}^{2-}$, suggesting its dependence on the presence of phosphate groups in each. Among all the phosphates studied, the quenching follows a trend, *viz.*, $\text{H}_2\text{PO}_4^- > \text{ATP}^{2-} \sim \text{HPO}_4^{2-} \sim \text{ADP}^{2-} > \text{AMP}^{2-} \gg \text{P}_2\text{O}_7^{4-}$ (Fig. 3d). All the data suggests that the cadmium complex is sensitive to phosphates, and it can be used further to differentiate H_2PO_4^- from the other phosphates studied because even low equivalents of this anion cause a major fluorescence quenching. The fluorescence quenching is considerable even at 20 ppb ($0.2 \mu\text{M}$) of H_2PO_4^- ,

whereas all other phosphates require a concentration of 50–580 ppb to cause the same effect on fluorescence spectra (Fig. 3c), suggesting that the interactive ability of H_2PO_4^- is higher by ~ 30 fold as compared to that of $\text{P}_2\text{O}_7^{4-}$ (ESI,† SI07). To understand the role of the counter cation, additional experiments were carried out in the presence of NaF, NaCl, NaBr, NaI, NaHSO₄ and NaClO₄; these compounds showed no change in the fluorescence intensity of the cadmium complex, suggesting that the presence of Na⁺ in place of the tetrabutyl ammonium counter cation played no significant role on the fluorescence intensity (ESI,† SI 08).

In the presence of phosphates, the fluorescent cadmium complex turns completely non-fluorescent, and the colour of the solution turns to that of L at different equivalents ranging from 2 to 12 from H_2PO_4^- to that of $\text{P}_2\text{O}_7^{4-}$, as can be seen from Fig. 3e. Thus, H_2PO_4^- is most interactive, whereas $\text{P}_2\text{O}_7^{4-}$ is the least. Thus, the fluorescence quenching is dependent on both the bulkiness of the organic moiety as well as the number of phosphate moieties present in the nucleotide, as observed from the corresponding study. The color change can be attributed to the release of L from its cadmium complex, in which the detached Cd^{2+} is stabilized by the corresponding phosphate through binding. Thus, the cadmium complex reported herein is well suited to differentiate phosphates from other anions and also to discriminate H_2PO_4^- and PPI from the other phosphates because their interacting abilities are the highest and lowest, respectively. Further, the interaction of the cadmium complex by phosphates is reversible, which was demonstrated by the successive addition of phosphates followed by Cd^{2+} for four cycles while observing its colour change and measuring the fluorescence intensity as demonstrated in the case of H_2PO_4^- (Fig. 3f). The differential quenching

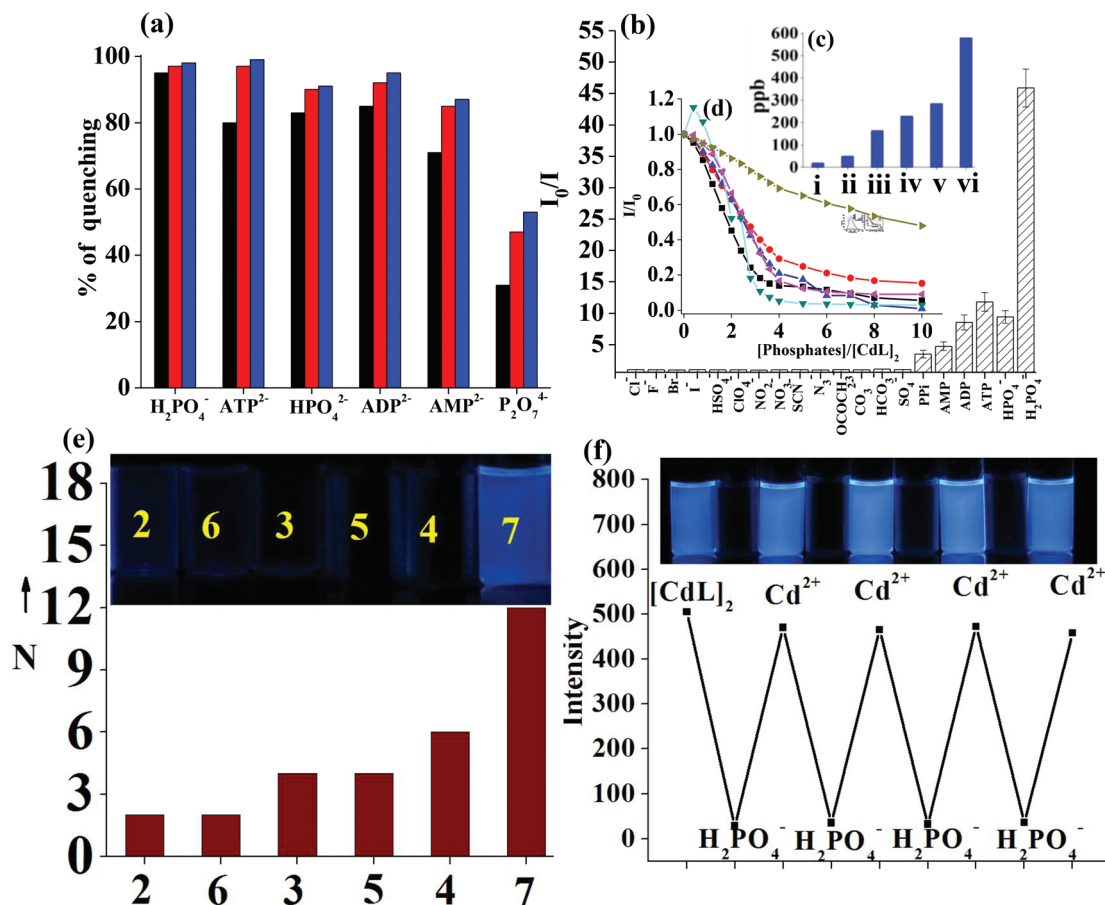


Fig. 3 (a) Histogram showing % fluorescence quenching with phosphates at different equivalents [colour code: black for 4 equiv.; red for 8 equiv.; blue for 10 equiv.] (b) Histogram showing the relative fluorescence intensity (I_0/I) of [CdL]₂ at 450 nm in the presence of various anions (Insets: (c) minimum detection limit for all phosphates i = H₂PO₄⁻, ii = HPO₄²⁻, iii = ATP²⁻, iv = ADP²⁻, v = AMP²⁻ and vi = PPI⁴⁻; (d) Relative fluorescence intensity (I/I_0) of [CdL]₂ with all the phosphates as a function of [Phosphates]/[CdL]₂ mole ratio. λ_{ex} = 370 nm. The colour code for the graphs in (d): black for ADP²⁻; red for AMP²⁻; blue for ATP²⁻; pink for HPO₄²⁻; olive for P₂O₇⁴⁻; cadet blue for H₂PO₄⁻. (e) Histogram showing the number of equivalents required for the complete quenching of fluorescence. (Inset: The visual color exhibited by the solution of cadmium complex in the presence of different anions under UV light [vial number, anion] [1, No anion]; [2, H₂PO₄⁻]; [3, HPO₄²⁻]; [4, AMP²⁻]; [5, ADP²⁻]; [6, ATP²⁻]; [7, P₂O₇⁴⁻] (N = number of equivalents require for complete quenching). (f) Relative fluorescence intensity (I/I_0) obtained during the titration of [CdL]₂ with H₂PO₄⁻ followed by the addition of Cd²⁺ (Inset: visual fluorescent colors after each addition of H₂PO₄⁻ followed by Cd²⁺ in a successive manner [CdL]₂ = 5 μ M; λ_{ex} = 370 nm).

pattern observed in the case of these phosphates has been addressed *via* the species formed, where the species were established based on ¹H NMR and mass spectrometry.

Absorption spectra

To support the results obtained from the fluorescence, absorption studies of the cadmium complex were carried out with different anions (ESI,† SI09). The complex shows the absorption band at 370 nm, which is attributed to the Cd²⁺-bound imino-phenolic core present in the conjugate.¹⁷ Due to the interaction of the complex with phosphates, including nucleotides, the absorbance of the ~370 nm band decreases, and a new band appears at ~326 nm along with a small shoulder at ~430 nm, which is the reminiscent of the presence of free L (Fig. 4). Among the phosphates, the order of the de-complexation follows a trend, H₂PO₄⁻ > ATP²⁻ > HPO₄²⁻ > ADP²⁻ > AMP²⁻ > P₂O₇⁴⁻ (insets of Fig. 4), as noticed based on the

quantitative changes observed in the absorbance of the bands, which is due to their pK_a values. To completely regenerate L from its cadmium complex, 3, 4, 5, 5, 6 and >10 equivalents of NaH₂PO₄, Na₂ATP, Na₂HPO₄, Na₂ADP, Na₂AMP and Na₄P₂O₇, respectively, are required, as obtained from the absorption studies. The new band at ~320 nm arises from the keto species that results from the keto-enol tautomerization in free L, which is otherwise prevented in the cadmium complex.¹⁷

¹H NMR spectra

To understand the interactive ability of phosphates with the cadmium complex and the consequent release of Cd²⁺ from it, ¹H NMR studies were carried out with sodium salts of phosphates, *i.e.* NaH₂PO₄, Na₂HPO₄, Na₄P₂O₇, Na₂AMP, Na₂ADP and Na₂ATP. During the study between the complex and NaH₂PO₄, it has been observed that the signals corresponding to the complex gradually diminishes, whereas the signals

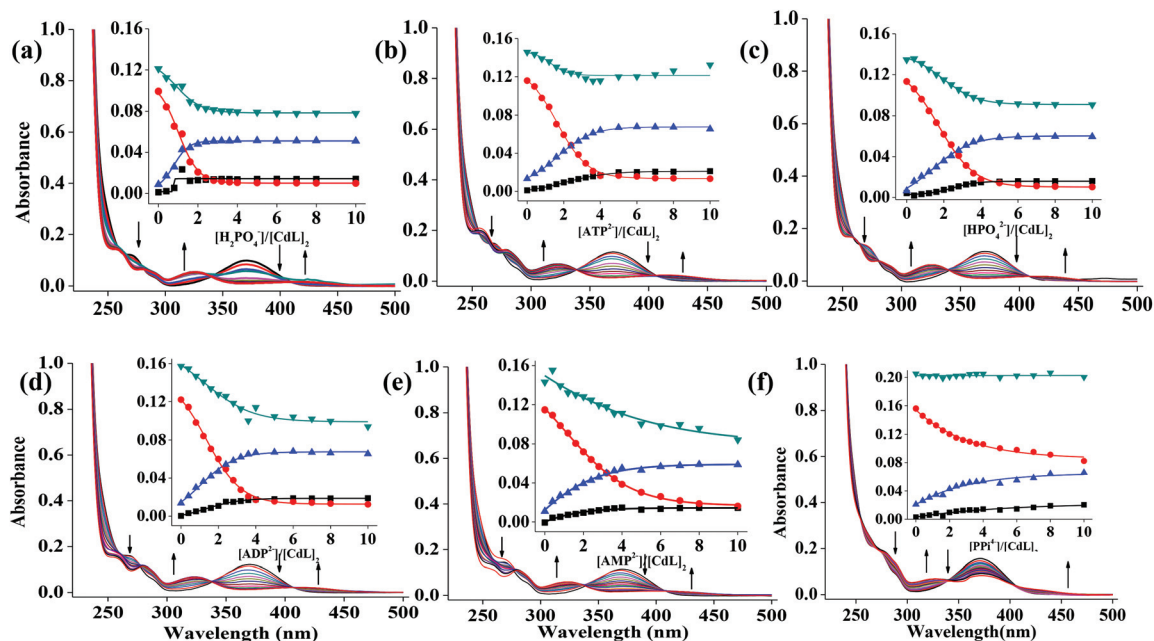


Fig. 4 Absorption spectra obtained during the titration of cadmium complex with phosphates: (a) for H_2PO_4^- ; (b) for ATP^{2-} ; (c) for HPO_4^{2-} ; (d) for ADP^{2-} ; (e) for AMP^{2-} ; and (f) for $\text{P}_2\text{O}_7^{4-}$. Inset in each case: Plots of absorbance vs. [phosphate ion]/ $[\text{CdL}_2]$ for different absorption bands. The colour code for the plots: black for 430 nm band; red for 370 nm band; blue for 320 nm band; cadet blue for 270 nm band.

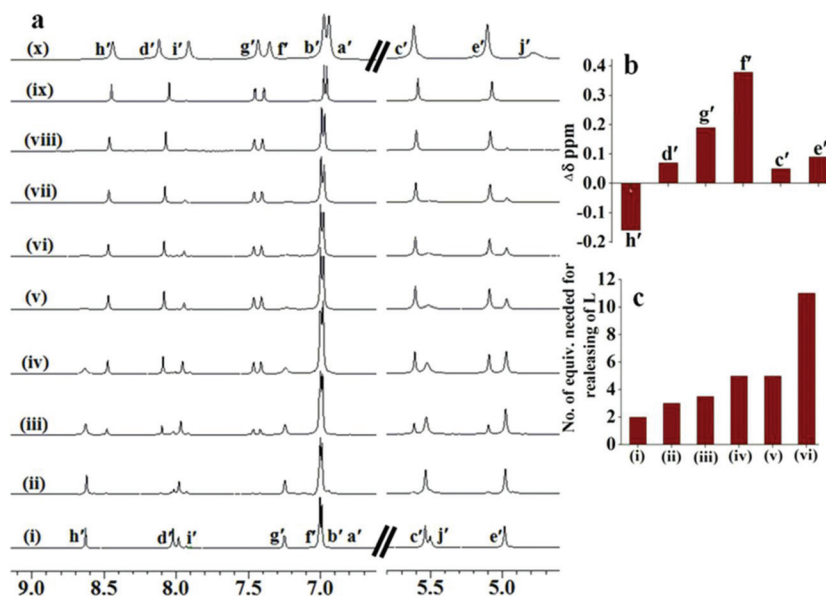


Fig. 5 (a) ^1H NMR spectral titration of $[\text{CdL}_2]$ with NaH_2PO_4 in $\text{DMSO}-d_6$: (i) $[\text{CdL}_2]$, $[\text{CdL}_2]$ followed by n equivalents of NaH_2PO_4 , where ' n ' is (ii) 0.1; (iii) 0.2; (iv) 0.3; (v) 0.5; (vi) 0.7; (vii) 0.9; (viii) 1.0; (ix) 1.5; (x) 2; and (x) 0 (simple L). (b) Histogram representing $\Delta\delta$ in the proton NMR peaks of the complex upon treatment with different phosphates (proton labeling is the same as that given in Fig. 1c). (c) Histogram showing the number of equivalents required for the release of L from $[\text{CdL}_2]$: (i) H_2PO_4^- ; (ii) ATP^{2-} ; (iii) HPO_4^{2-} ; (iv) ADP^{2-} ; (v) AMP^{2-} and (vi) PPI^{4-} .

corresponding to free L start appearing with increasing concentration of NaH_2PO_4 , and L is completely regenerated around two equivalents, clearly suggesting the release of L from the complex, *viz.*, $[\text{CdL}_2]$ (Fig. 5a). A similar study carried out with different phosphates exhibited the complete regeneration of L at different equivalents ranging from 2 to 11 from

NaH_2PO_4 to $\text{Na}_4\text{P}_2\text{O}_7$, as can be seen from Fig. 5c (ESI,† SI10). Thus, the order of releasing L from the cadmium complex among the inorganic phosphates is $\text{H}_2\text{PO}_4^- > \text{HPO}_4^{2-} > \text{P}_2\text{O}_7^{4-}$, and among the nucleotides, this follows a trend, $\text{ATP}^{2-} > \text{ADP}^{2-} > \text{AMP}^{2-}$. These results clearly suggest that the H_2PO_4^- can de-chelate Cd^{2+} more efficiently from its complex as com-

pared to the other phosphates studied. The protons of c', d', e', f', and g' show a downfield shift, whereas that of h' shows an upfield shift, but to different extents (Fig. 5b). All these shifted proton resonances correspond to that of L, suggesting the release of free L from the cadmium complex. The -OH resonances could not be monitored due to their exchange with D₂O.

ESI MS spectra

To provide further support for the binding of phosphates followed by the removal of Cd²⁺ from its complex, ESI MS studies were carried out. The spectra obtained in the case of H₂PO₄⁻ initially shows the formation of a protonated ternary species, as observed from the peak in the mass spectrum at *m/z* of 1523.67 (CdL + H₂PO₄ + K + H)⁺ along with the *m/z* peak for free L at 1299.76 (L + Na)⁺ (Fig. 6). The H₂PO₄⁻-bound cadmium species was observed at the *m/z* of 413.26 (Cd + 3H₂PO₄ + Li + H)⁺, and this is further confirmed by the presence of the isotopic peak pattern of cadmium. The studies clearly demonstrate the initial binding of H₂PO₄⁻ at the cadmium center, resulting in a ternary species followed by the removal of Cd²⁺. The intensity of the peak corresponding to the L in ESI MS increases with the concentration of the added H₂PO₄⁻.

Similar studies carried out with other phosphates *viz.*, HPO₄²⁻, P₂O₇⁴⁻, ATP²⁻, ADP²⁻ and AMP²⁻, resulted in ternary species possessing the respective phosphate, and the corresponding mass spectral peaks are observed at the *m/z* of

1522.56 (CdL + HPO₄ + K + 2H)⁺, 1579.67 (CdL + P₂O₇ + 2Li + 3H)⁺, 1939.14 (CdL + ATP + 3H)⁺, 1888.08 (CdL + ADP + 2 K + H)⁺, 1747.64 (CdL + AMP + 2Li + H)⁺ (Fig. 7). In addition, all the spectra showed *m/z* peaks corresponding to free L. These results suggest that the phosphates initially bind to the cadmium center to form ternary species, before the Cd²⁺ is being taken out of the complex as its phosphate (ESI, ‡ SI11).

Computational modeling of the ternary species

As the ternary species formation between the cadmium complex and the phosphates were shown by ESI MS, the computational studies were carried out to model them and reveal their structural features. The computational studies are carried out in the cases of six different phosphates, X (X = H₂PO₄⁻, HPO₄²⁻, PPI⁴⁻, AMP²⁻, ADP²⁻ and ATP²⁻). The initial model of [CdL]₂ was taken from the structure obtained from the single crystal XRD (Fig. 2) and was used for the complexation with each of the six phosphates. The cadmium center for the minimized structure of [CdLX]₂ showed coordination through the phosphate oxygens of X. The coordination of the -CH₂-CH₂-OH groups to the metal center is detached as these were pushed away from the Cd²⁺ center by the incoming phosphate to a distance of 3.3 to 5.2 Å, and this appears to depend upon the extent of the interaction exhibited by X, whereas the same shows 2.4 to 2.5 Å prior to X binding, which occurs at both the cadmium centers. As a result of the displacement of the bound -CH₂-CH₂-OH, the phosphate (X) enters into the

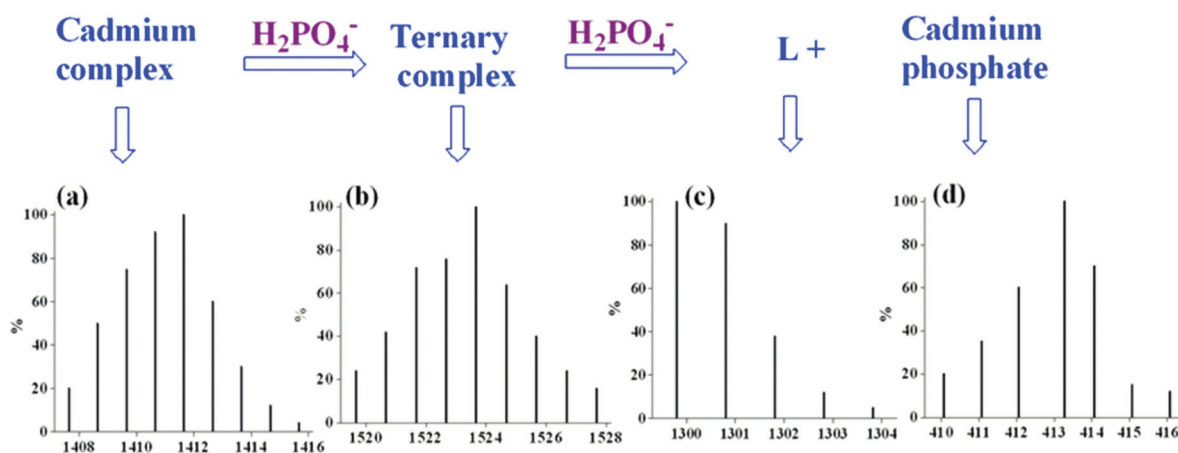


Fig. 6 ESI MS study with NaH₂PO₄: (a) [CdL]₂; (b) ternary species; (c) L; (d) cadmium phosphate adduct.

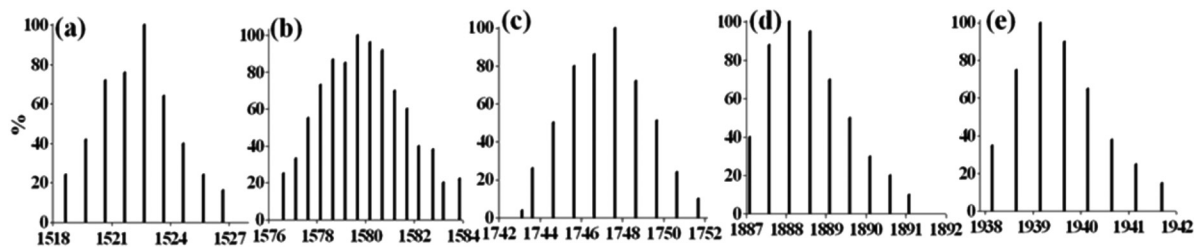


Fig. 7 Ternary complex formed between [CdL]₂ and phosphate in ESI MS titration: (a) HPO₄²⁻; (b) P₂O₇⁴⁻; (c) AMP²⁻; (d) ADP²⁻; (e) ATP²⁻.

primary coordination domain of the Cd^{2+} center at a $\text{Cd}^{2+}\cdots\text{O}_x$ distance of 2.0 to 2.1 Å. This fulfils six coordination sites, and the cadmium geometry is restored back to the distorted octahedral upon binding to phosphate. In the ternary species, the $\text{Cd}-\text{O}_{\text{phenolic}}$ and the $\text{Cd}-\text{N}$ distances are shortened by 0.15 to 0.20 Å, suggesting a strong link that persists between **L** and the cadmium center. However, in the minimized structures of the ternary species, *viz.*, $[\text{CdLX}]_2$, the coordination spheres show varying binding behaviors depending upon the nature of the phosphate (**X**) involved, and the same can be seen from Fig. 8 (ESI,† SI10). In the phosphate-bound ternary complexes, the Cd1, exhibits *trans*-angles in the range of 153°–174° and the other angles in the range of 72°–113°, whereas Cd2

exhibits *trans*-angles in the range of 140°–173° and the other angles in the range of 67°–122°, supporting the distorted octahedral geometry around both the cadmium centers. This is the same in all the phosphate-based ternary species, *viz.*, $[\text{CdLX}]_2$ studied herein.

The *trans*-like angle observed in the cadmium crystal structure turns *cis*-like in its ternary species formed with the incorporation of the phosphate. Moreover, at the Cd2 center, this angle is 129° in the crystal structure, and it turns to *trans*-like in its ternary species formed by the phosphates of HPO_4^{2-} , H_2PO_4^- and $\text{P}_2\text{O}_7^{4-}$ and *cis*-like in the case of AMP^{2-} , ADP^{2-} and ATP^{2-} . This suggests that the nature of the interaction of these phosphates with the cadmium center plays a significant role (ESI,† SI11–SI16). Thus, the Cd2 center in this complex differentiates the inorganic phosphates from those of the biological ones. In the case of the angle O008–Cd1–O008 at the Cd1 center, it is exactly opposite to what was observed with the N00C–Cd1–N00C. However, the angle of O005–Cd2–O005 at Cd2 center does not alter on going from the crystal structure to that of the ternary species. In all the ternary species, the phosphates act as bidentate ligands. The distance between the two cadmium centers change from 5.5 to 8.1 to 9.5 Å on going from the crystal structure to the H_2PO_4^- to the ATP^{2-} binding. This suggests the effect of bulkiness of the ATP^{2-} on the structural features of the ternary species, and hence the release of Cd^{2+} is easier in this case. As a result of all these changes occurring in the coordination sphere, including that of the geometry, the adenosine moiety of the biological phosphates extends into the vicinity by weakening the cadmium core (Fig. 9).

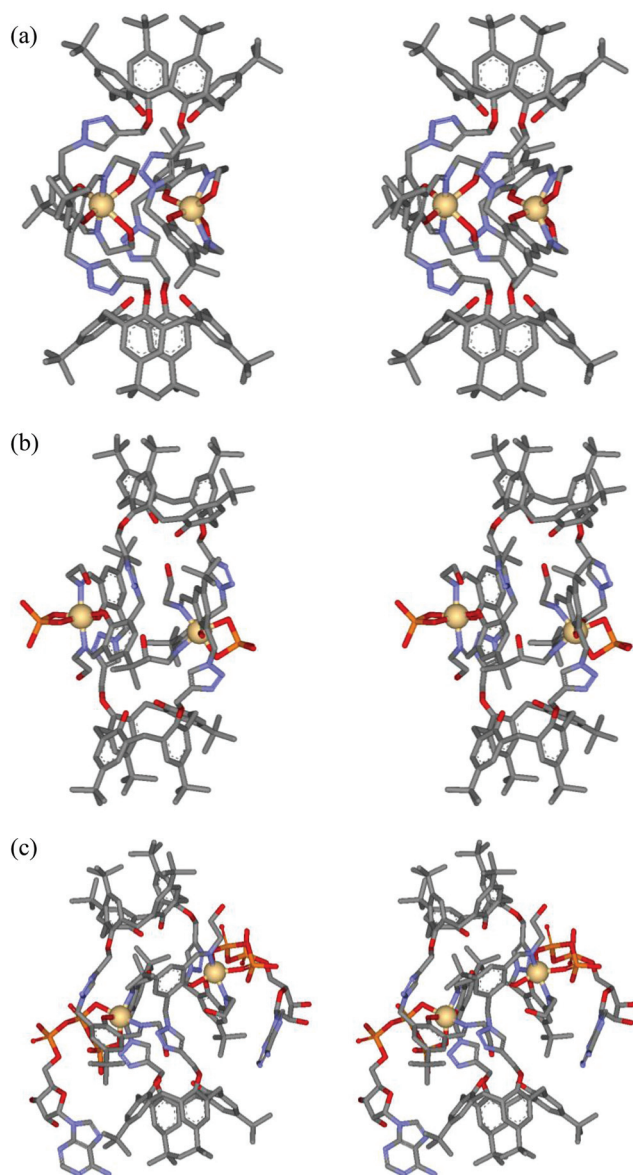


Fig. 8 Stereo views of the crystal structure of the di-cadmium complex and its phosphate-bound ternary complexes obtained through MM minimization: (a) crystal structure of $[\text{CdL}]_2$, (b) $[\text{CdLH}_2\text{PO}_4^-]_2$ and (c) $[\text{CdLATP}^{2-}]_2$.

Fluorescence microscopy studies with HeLa cells

To show the practical utility of the cadmium complex for the detection of H_2PO_4^- present in the biological medium, fluorescence microscopy studies were carried out using HeLa cells. After incubating the cells for 24 hours, the medium was replaced with PBS buffer (pH = 7.4) containing 20 μM of the conjugate (**L**), and further incubated for 20 min at 37 °C and 5% CO_2 . The cells were washed with the same buffer to remove excess of **L**. At this stage, the HeLa cells displayed very low intracellular fluorescence (Fig. 10a–d). Upon the addition of 20 μM Cd^{2+} to these cells exogenously *via* incubation with Cd^{2+} /pyrithione (1 : 1) solution for 20 min at 37 °C, the cells exhibited highly intense blue fluorescence (Fig. 10e–h). Differential interference contrast microscopy (DIC) measurements for each experiment confirmed that the cells were viable throughout the imaging experiments, and the merged images supported the fact that the fluorescence was emerging through the cells. However, when **L** and Cd^{2+} /pyrithione pre-incubated HeLa cells were further treated with H_2PO_4^- for 20 min at 37 °C, the fluorescence intensity was quenched, as can be observed from the microscopy images (Fig. 10i–l). The fluorescence emission is at least seven times higher in the presence of $[\text{L} + \text{Cd}^{2+}]$ in the HeLa cells as compared to those incubated only with **L**. However, in the presence of H_2PO_4^- , the fluorescence enhancement is only about two times that of **L**, suggesting that the

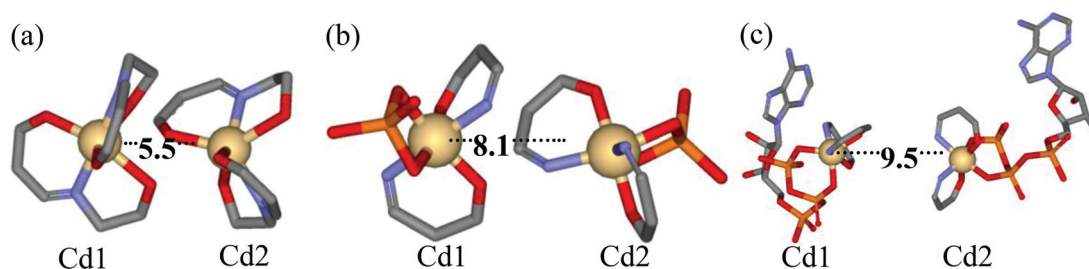


Fig. 9 The coordination spheres: (a) crystal structure of $[\text{CdL}]_2$; (b) ternary species, $[\text{CdLH}_2\text{PO}_4^-]_2$; and (c) ternary species, $[\text{CdLTP}^{2-}]_2$. The distances (in Å) between the cadmium centers are given in the figure.

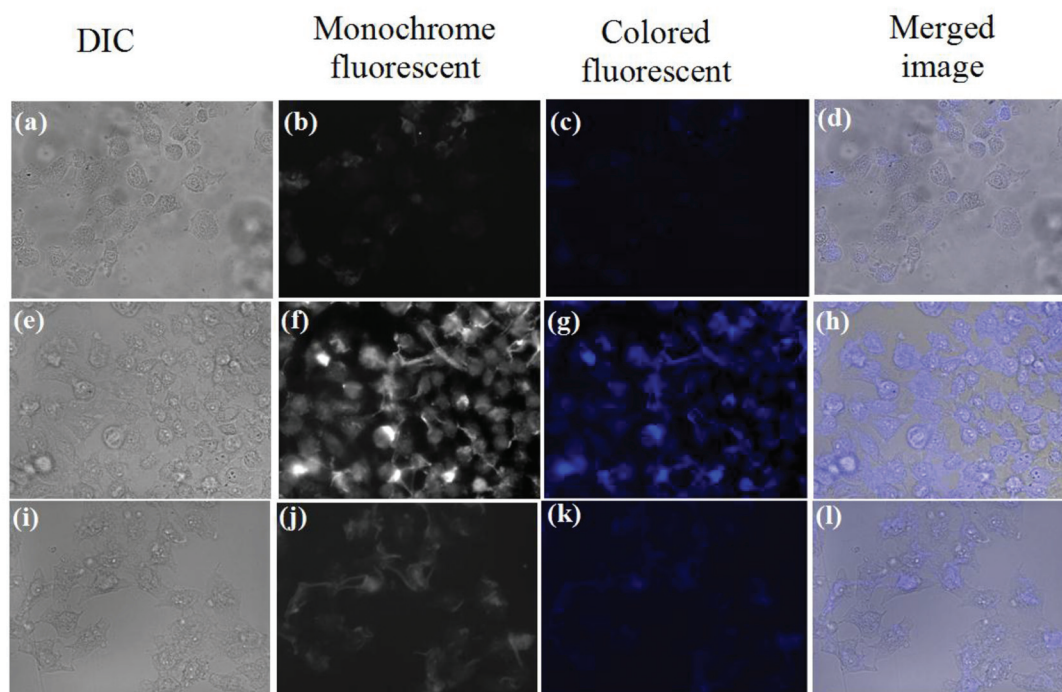


Fig. 10 Fluorescence images obtained at 40 \times magnification from the HeLa cells (excitation at λ_{max} 358 nm and emission at λ_{max} 461 nm) upon treatment in PBS buffer at pH = 7.4: (a) DIC image when treated with L (20 μM); (b) monochrome fluorescence of (a); (c) fluorescence image of (a); (d) a merge image of (a) and (c). (e) DIC image of HeLa cells treated with L followed by 20 μM of Cd^{2+} -Pyrrithione (1 : 1) solution; (f) monochrome fluorescence of (e); (g) fluorescence image (e); (h) a merge image of (e) and (g). (i) DIC microscopy image of the HeLa cells treated with [L + Cd^{2+} -Pyrrithione(1 : 1)] followed by 80 μM of H_2PO_4^- ; (j) monochrome fluorescence of (i); (k) fluorescence image (j); (l) a merge image of (i) and (k).

fluorescence is quenched in HeLa cells in the presence of H_2PO_4^- (ESI,† SI19). Therefore, the cellular studies clearly indicate that the conjugate **L** exhibits cell permeability and shows effective intracellular fluorescence emission through forming an *in situ* complex, which in turn loses its fluorescence intensity upon treatment with H_2PO_4^- .

Conclusions and correlations

The hydroxyethylimino-based triazole-linked calix[4]arene conjugate **L** has been synthesized and characterized. A dinuclear Cd^{2+} complex of **L**, *i.e.*, $[\text{CdL}]_2$ has been isolated and was characterized by various spectroscopic and analytical techniques. The structure of the di-nuclear cadmium complex has been established by single crystal XRD. In the crystal structure, both the cadmium centers were bound by a N_2O_4 core that is

supported by **L** using two phenolic oxygens, two imine nitrogens and two terminal ethanolic oxygens. The isolated dinuclear cadmium complex has high fluorescence emission at 450 nm when excited at 380 nm through exhibiting intense blue color fluorescence under UV light. Owing to this unique feature of the cadmium complex, the interaction of anions, in particular the phosphates were studied. The interaction of H_2PO_4^- was well demonstrated using various techniques, *viz.*, fluorescence, absorption, visual color change, ^1H NMR, ESI MS, computational modeling and cell imaging by fluorescence microscopy.

The quenching of the fluorescence intensity of the cadmium complex by phosphates followed an order, *viz.*, $\text{H}_2\text{PO}_4^- \gg \text{ATP}^{2-} > \text{HPO}_4^{2-} > \text{ADP}^{2-} > \text{AMP}^{2-} > \text{P}_2\text{O}_7^{4-}$. A 50% fluorescence quenching is observed at ~ 2 equiv. in the case of

H_2PO_4^- , ~ 2.5 equiv. in case of ATP^{2-} , HPO_4^{2-} and ADP^{2-} , and ~ 10 equiv. in case of $\text{P}_2\text{O}_7^{4-}$. The observed difference in the quenching effects reflects their differential interactive ability. The fluorescence quenching is considerable even at 20 ppb (0.2 μM) of H_2PO_4^- , whereas all the other phosphates require a concentration of 50–580 ppb to bring the same effect on fluorescence spectra. Thus, the interactive ability of H_2PO_4^- is higher by ~ 30 times as compared to that of $\text{P}_2\text{O}_7^{4-}$.

During the interaction, H_2PO_4^- initially forms a ternary species containing Cd^{2+} , **L** and H_2PO_4^- , followed by the removal of Cd^{2+} from this complex, which is being further stabilized through the formation of a cadmium–phosphate adduct. The presence of cadmium in the ternary species and also in the cadmium–phosphate adduct have been confirmed by observing the isotopic peak pattern expected for cadmium in ESI MS. These features were further confirmed by ^1H NMR studies. The formation of ternary species between **L**, cadmium and the phosphate has been addressed by computational modeling, which was carried out using all the six phosphates. In the optimized structures of the ternary species, both the Cd^{2+} centers occupy distorted octahedral geometry by bonding through two phenolate oxygens, two imine nitrogens and two phosphate oxygens, resulting in an N_2O_4 binding core at each of the cadmium centers. This also results in removing the bound $-\text{CH}_2-\text{CH}_2-\text{OH}$ groups from the primary coordination spheres of the cadmium centers. The $\text{Cd}\cdots\text{Cd}$ distance change from 5.5 to 8.1 to 9.4 Å on going from the crystal structure to the H_2PO_4^- to the ATP^{2-} bound species, suggesting the influence of the bulkiness of the ATP^{2-} on the structural features of the ternary species, and therefore the release of Cd^{2+} is easier in this case. The practical utility of the complex was shown by HeLa cells using fluorescence microscopy, which would be useful in cellular imaging.

Thus, the present paper demonstrates the differential interactive abilities of phosphates by monitoring the spectral changes of a structurally characterized di- Cd^{2+} complex of calix[4]conjugate *via* the formation of ternary species, and the utility of the cadmium complex in cell imaging. When the terminal $-\text{CH}_2-\text{CH}_2-\text{OH}$ group is being replaced by $-\text{CH}_2-\text{CH}_2-\text{N}(\text{CH}_3)_2$, the resultant calix-conjugate yields a mono-nuclear cadmium complex, and the corresponding complex interacts with Cys, as reported recently by us.^{7a}

Experimental section

General information and materials

The acetate salt of metal $\text{Cd}(\text{CH}_3\text{COO})_2\cdot 2\text{H}_2\text{O}$ and the tetrabutylammonium and sodium salts of different anions, *viz.*, Bu_4NF , Bu_4NCl , Bu_4NBr , Bu_4NI , Bu_4NClO_4 , Bu_4NHSO_4 , NaH_2PO_4 , Na_2HPO_4 , $\text{Na}_4\text{P}_2\text{O}_7$, NaSCN , Na_2SO_4 , Na_2CO_3 , NaHCO_3 , NaNO_3 , NaNO_2 , NaN_3 , Na_2AMP , Na_2ADP and Na_2ATP , were procured from the commercial suppliers. All the solvents used were procured from local sources and were dried and distilled by usual procedures immediately before use. All the fluorescence titrations were carried out in 1 cm quartz cells using

25 μL of **L**, and the total volume in each measurement was made to 3 mL to obtain a final concentration of the ligand as 5 μM . The fluorescence and absorption studies were performed in ethanol as a solvent. NMR spectra were recorded on an Avance III-400 (Bruker) NMR spectrometer. IR spectra were recorded by preparing KBr pellets, using a Perkin Elmer spectrum one FTIR spectrometer. Mass spectra were recorded using micromass Q-ToF micro.

Synthesis and characterization of P

The dipropargyl derivative calix[4]arene (3.0 g, 4.14 mmol) was added to a solution of 3-(azidomethyl)-5-(*tert*-butyl)-2-hydroxybenzaldehyde (2.12 g, 9.53 mmol) in 100 mL mixture of dichloromethane and water (50:50). To this solution, $\text{CuSO}_4\cdot 5\text{H}_2\text{O}$ (0.12 g, 0.50 mmol) and sodium ascorbate (0.34 g, 1.70 mmol) were added. The resulting solution was stirred for 12 hrs at room temperature. Upon completion of the reaction as checked by TLC, the organic layer was separated, and the aqueous layer was extracted with dichloromethane (2 \times 50 mL). The combined organic layer was washed with water and then with brine (2 \times 100 mL) and dried over anhydrous Na_2SO_4 , and the solvent was removed under *vacuo*. The crude product was purified by triturating with hexane, followed by filtering the precipitate. Yield, 89.91%. ^1H NMR (CDCl_3 , 400 MHz) δ (ppm): 11.30 (s, 2H), 9.83 (s, 2H), 8.08 (s, 2H), 7.62 (s, 2H) 7.49 (d, 2H), 7.15 (s, 2H), 6.98 (s, 4H), 6.77 (s, 4H), 5.56 (s, 2H), 5.18 (s, 2H), 4.14 (d, $J = 13.0$ Hz, 4H), 3.17 (d, $J = 13.0$ Hz, 4H), 1.27 (s, 18H), 1.26 (s, 18H), 0.96.¹³C NMR (CDCl_3 , 100 MHz) δ (ppm): 196.6, 157.1, 150.4, 149.6, 147.2, 144.2, 143.2, 141.5, 135.3, 132.6, 130.7, 127.8, 125.6, 125.0, 124.2, 123.1, 120.2, 69.8, 48.2, 34.2, 33.9, 33.8, 31.7, 31.2, 31.1, 31.02. IR: $\nu = 3463, 2959, 1656, 1483, \text{cm}^{-1}$. HRMS (ESI) calcd for $\text{C}_{74}\text{H}_{90}\text{N}_6\text{O}_8$ $[\text{M} + \text{H}]^+$: 1191.6898, found 1191.6898.

Synthesis and characterization of L

The mixture of **1** (0.50 g, 0.42 mmol) and ethanol amine (0.13 g, 2.1 mmol) in 20 mL methanol was refluxed for 12 h. A faint yellow precipitate was observed upon completion of the reaction. The precipitate was filtered to obtain a yellow solid product. Yield 93%. ^1H NMR (CDCl_3 , 400 MHz, δ ppm): 0.97 (s, 18H, $-\text{C}(\text{CH}_3)_3$), 1.20 (s, 18H, $-\text{C}(\text{CH}_3)_3$), 1.25 (s, 18H, $-\text{C}(\text{CH}_3)_3$), 3.19 (d, 4H, $\text{Ar}-\text{CH}_2\text{eq}-\text{Ar}$, $J = 12.8$), 3.66 (t, 4H, $-\text{N}-\text{CH}_2$, $J = 4.32$), 3.88 (t, 4H, $-\text{O}-\text{CH}_2$, $J = 4.32$), 4.12 (d, $\text{Ar}-\text{CH}_2\text{ax}-\text{Ar}$, $J = 12.8$), 5.11 (s, 4H, $\text{Ar}-\text{CH}_2$ -triazole), 5.38 (s, 4H, $\text{Ar}-\text{O}-\text{CH}_2$), 6.79 (s, 4H, $\text{Ar}-\text{H}$). 6.97 (s, 4H, $\text{Ar}-\text{H}$), 7.21 (d, 2H, $\text{Ar}-\text{H}$, $J = 2.4$), 7.36 (d, 2H, $\text{Ar}-\text{H}$, $J = 2.4$), 8.18 (s, 2H, triazole-H), 8.32 (s, 2H, imine-H). ¹³C NMR (CDCl_3 , 100 MHz, δ ppm): 31.17, 31.36 ($-\text{C}(\text{CH}_3)_3$), 31.46, 31.84 ($-\text{C}(\text{CH}_3)_3$), 32.00, 33.97 ($-\text{C}(\text{CH}_3)_3$), 34.11, 34.13 ($\text{Ar}-\text{CH}_2-\text{Ar}$), 48.67 ($\text{Ar}-\text{CH}_2$), 61.79 ($-\text{NCH}_2$), 61.88 ($-\text{O}-\text{CH}_2$), 70.29 ($-\text{OCH}_2$), 118.20, 122.03, 123.83, 124.03, 125.19, 125.85, 127.78, 128.91, 130.81, 132.75, 141.35, 141.74, 144.51, 147.42, 149.90, 150.57, 157.78, 166.73 $\text{Ar}-\text{C}$. HRMS (ESI) calcd for $\text{C}_{78}\text{H}_{101}\text{N}_8\text{O}_8$ $[\text{M} + \text{H}]^+$: 1277.7742, found 1277.7708. FTIR (KBr, cm^{-1}): 1638 ($\nu_{\text{C}=\text{N}}$), 2961 ($\nu_{\text{C}-\text{H}}$), 3421 (ν_{OH}).

Synthesis and characterization of cadmium complex

A solution of **L** (0.20 g, 0.15 mmol) and $\text{Cd}(\text{CH}_3\text{COO})_2 \cdot 2\text{H}_2\text{O}$ (0.050 g, 0.18 mmol) in methanol was refluxed for 12 h. After concentrating the solution, a faint yellow, off-white precipitate was observed, and the solid formed was then filtered, washed with methanol, and dried under vacuum to obtain the desired product. [CdL]: (Yield, 55%), $^1\text{H NMR}$ ($\text{DMSO}-d_6$, 400 MHz, δ ppm): 1.08 (s, 18H, $-\text{C}(\text{CH}_3)_3$), 1.16 (s, 18H, $-\text{C}(\text{CH}_3)_3$), 1.21 (s, 18H, $-\text{C}(\text{CH}_3)_3$), 3.06 (d, 4H, $\text{Ar}-\text{CH}_2\text{eq}-\text{Ar}$, $J = 15.6$), 3.45 (br, 4H, $-\text{N}-\text{CH}_2$), 3.59 (br, 4H, $-\text{N}-\text{CH}_2$), 3.90 (d, $\text{Ar}-\text{CH}_2\text{ax}-\text{Ar}$, $J = 15.2$), 4.98 (s, 4H, $\text{Ar}-\text{CH}_2$ -triazole), 5.53 (s, 4H, $\text{Ar}-\text{O}-\text{CH}_2$ & 2H, $\text{OH}-\text{CH}_2-$), 7.00 (s, 8H, $\text{Ar}-\text{H}$ & 2H, $\text{Sal}-\text{H}$), 7.25 (s, 2H, $\text{Sal}-\text{H}$), 7.98 (s, 2H, $\text{Ar}-\text{OH}$), 8.02 (s, 2H, triazole-H), 8.63 (s, 2H, imine-H). $^{13}\text{C NMR}$ ($\text{DMSO}-d_6$, 100 MHz, δ ppm): 31.08, 31.6231.75, 31.92 ($-\text{C}(\text{CH}_3)_3$), 31.98, 32.31, 33.78 ($-\text{C}(\text{CH}_3)_3$), 33.85, 33.89, 33.97 ($-\text{C}(\text{CH}_3)_3$), 34.03, 34.06 ($\text{Ar}-\text{CH}_2-\text{Ar}$), 52.06 ($\text{Ar}-\text{CH}_2$), 60.59 ($-\text{NCH}_2$), 61.22 ($-\text{O}-\text{CH}_2$), 62.24 ($\text{HO}-\text{CH}_2-$), 69.15 ($-\text{OCH}_2$), 118.80, 120.32, 123.30, 125.01, 125.11, 125.44, 125.62, 125.85, 126.53, 127.67, 127.93, 128.13, 128.30, 128.50, 131.11, 131.45, 132.74, 132.83, 133.10, 133.68, 133.89, 134.03, 137.98, 141.74, 143.63, 144.06, 146.63, 147.39, 150.50, 150.60, 166.31, 170.00, 170.68, 171.30 $\text{Ar}-\text{C}$. **ESI MS (ESI)** calcd for $\text{C}_{156}\text{H}_{196}\text{N}_{16}\text{O}_{16}\text{Cd}_2$ [M] $^+$: 15% found 2776.41, and [$\text{M}/2$] $^+$: 100% found 1389.57. **FTIR** (KBr, cm^{-1}): 1645 ($\nu_{-\text{C}=\text{N}}$), 2925 ($\nu_{-\text{C}-\text{H}}$), 3398 ($\nu_{-\text{OH}}$). **Anal. Calcd** for $\text{C}_{156}\text{H}_{204}\text{N}_{16}\text{O}_{20}\text{Cd}_2$: Calcd C 65.78%; H 7.22%; N 7.87% Found C 65.84%; H 7.15%; N 7.32%.

Crystallographic details

Because the single crystals of the cadmium complex obtained from $\text{DMSO}-\text{CHCl}_3$ mixture are sensitive to moisture, these were immediately covered with oil upon removal from the mother liquor. The suitable crystals were sorted on a microscope plate, and the selected crystal was then mounted on a goniometer. The mounted crystal was cooled under a stream of liquid nitrogen to a temperature of 100 K and was maintained in the jet of liquid nitrogen flow. The diffraction data were collected using a graphite monochromator ($\lambda = 0.71073^\circ$) on a Rigaku Saturn CCD diffractometer, which was connected to an Oxford cryo-systems cooler device. The unit cell was determined, and a complete data emerging from one hemisphere were collected, and the data were reduced while performing all these using Rigaku Crystal Clear-SM Expert 2.1 software. About one-fourth of this data turns out to be unique reflections, and the unique data were used to solve the structure by direct methods using SHELXTL package on a desktop computer. The total structure was obtained by carrying out four iterative cycles of Fourier-difference Fourier successively. Integrated intensities of the collected data were obtained using SAINT^{18a}, and the data were subjected to numerical absorption correction using SADABS.^{18b} The structure was refined using full matrix least-squares procedures on F^2 with SHELXTL package.^{18c} Because the solvent molecules were heavily disordered within the lattice, the electron density corresponding to these could not be modeled, and hence the SQUZEE facility

from PLATON^{18d} was used, which resulted in a smooth refinement of the structure. Two-thirds of the *t*-butyl groups present in the structure were disordered, and these were modeled and isotropically refined for better convergence during the refinement process. To model the disorder of *t*-butyl groups, several restraints and constraints, such as SIMU and DFIX, were employed. All the hydrogen atoms, except the coordinated alcoholic-OH and the coordinated water, were geometrically fixed and refined as riding atoms on their bound heavier ones. The residual electron density loop of the disordered solvent that was generated by the PLATON was appended to the cif file. The final structure was refined by Olex2.

Crystal data of the complex, [CdL]₂. Empirical formula – $\text{C}_{156}\text{H}_{196}\text{N}_{16}\text{O}_{16}\text{Cd}_2$, Formula weight – 2776.08, Temperature (K) – 100(2), Crystal System – Monoclinic, Space group – $I2/a$, $a/\text{\AA}$ – 33.44(9), $b/\text{\AA}$ – 16.05(4), $c/\text{\AA}$ – 43.090(10), $\alpha/^\circ$ – 90.00, $\beta/^\circ$ – 101.89(5), $\gamma/^\circ$ – 90.00, Volume/ \AA^3 – 22 631, Z – 4, Absorption Coefficient (mm^{-1}) – 0.232, Density – 0.816 Mg m^{-3} , Reflections collected – 89 101, Independent reflections – 21 370, Parameters – 850, R_{int} – 0.0822, Final R ($I > 2\sigma(I)$) – 0.0976, wR_2 – 0.2982.

Computational studies

To understand the interactions present between $[\text{CdL}]_2$ and the phosphate-based species, computational studies were carried out using molecular mechanics methods using ArgusLab^{16,19} software. To make the $[\text{CdLX}]_2$ complexes of $[\text{CdL}]_2$ with phosphate possessing species ($\text{X} = \text{H}_2\text{PO}_4^-$, HPO_4^{2-} , PPi^{4-} , AMP^{2-} , ADP^{2-} and ATP^{2-}), further computational studies were carried out by keeping the phosphate near each Cd^{2+} centre using the DS visualizer and minimized. All the MM calculations were carried out using ArgusLab with UFF, and the steepest descent method (Gradient convergence = 0.1 $\text{kcal mol}^{-1} \text{\AA}^{-1}$) was used for the minimization.

Acknowledgements

CPR acknowledges the financial support from DST, CSIR and DAE-BRNS. VVSM acknowledges CSIR for SRF. We are grateful to Professor Maheswaran Shanmugam for helping us with the X-ray structure. We thank Mr Rajeev Chandan for helping us with the cell studies and Mr Gowri Naidu for some spectral help. We thank the crystallography reviewer for helping us with the structure.

References

- (a) A. E. Hargrove, S. Nieto, T. Zhang, J. L. E. V. Sessler and Anslyn, *Chem. Rev.*, 2011, **111**, 6603; (b) R. L. P. Adams, J. T. Knowler and D. P. Leader, *The Biochemistry of the Nucleic Acids*, Chapman and Hall, New York, 10th edn, 1986; (c) W. Saenger, *Principles of Nucleic Acid Structure*, Springer-Verlag, New York, 1984; (d) F. J. J. McClure, *Dent. Res.*, 1950, **29**, 315; (e) O. G. Tsay, S. T. Manjare, H. Kim, K. M. Lee, Y. S. Lee and D. G. Churchill, *Inorg. Chem.*, 2013,

- 52, 10052; (f) S. Khatua, S. H. Choi, J. Lee, K. Kim, Y. Do and D. G. Churchill, *Inorg. Chem.*, 2009, **48**, 2993.
- 2 (a) C. K. Mathews and K. E. V. Holde, *Biochemistry*, Benjamin/Cummings, CA, 1990; (b) S. N. Jackson, H. J. Wang, A. Yergey and A. S. Woods, *J. Proteome Res.*, 2006, **5**, 122; (c) A. Kumar, S. Mehtab, U. P. Singh, V. Aggarwal and J. Singh, *Electroanalysis*, 2008, **20**, 1186; (d) S. K. Kim, D. H. Lee, J.-I. Hong and J. Yoon, *Acc. Chem. Res.*, 2009, **42**, 23; (e) M. Choi, M. Kim, K. D. Lee, K.-N. Han, I.-A. Yoon, H.-J. Chung and J. Yoon, *Org. Lett.*, 2001, **3**, 3455.
- 3 (a) E. Takeda, Y. Taketani, N. Sawada, T. Sato and H. Yamamoto, *Biofactors*, 2004, **21**, 345; (b) B. P. Morgan, S. He and R. C. Smith, *Inorg. Chem.*, 2007, **46**, 9262.
- 4 (a) C.-P. Li, H. R. Ibrahim, Y. Sugimoto, H. Hatta and T. Aoki, *J. Agric. Food Chem.*, 2004, **52**, 5752; (b) P. K. Datta, A. C. Frazer, M. Sharratt and H. G. Sammons, *J. Sci. Food Agric.*, 1962, **13**, 556; (c) M. Peld, K. Tonsuaadu and V. Bender, *Environ. Sci. Technol.*, 2004, **38**, 5626; (d) S. R. Dar, T. Thomas, J. C. Dagar, K. Lal, A. H. Mir, A. Kumar, H. Mir, M. R. Bakshi, S. Mehboob and D. Singh, *Afr. J. Agric. Res.*, 2012, **7**, 4996.
- 5 J. E. McLean and B. E. Bledsoe, *Behavior of Metals in Soils*, EPA/540/S-92/018 October 1992.
- 6 (a) C. Buzea, I. I. P. Blandino and K. Robbie, *Biointerphases*, 2007, **4**, MR17; (b) A. F. A. Peacock and V. L. Pecoraro, *Cadmium: From Toxicity to Essentiality Metal Ions in Life Sciences*, 2013, **11**, 303.
- 7 (a) R. K. Pathak, V. K. Hinge, K. Mahesh, A. Rai, D. Panda and C. P. Rao, *Anal. Chem.*, 2012, **84**, 6907; (b) R. Joseph and C. P. Rao, *Chem. Rev.*, 2011, **111**, 4658; (c) J. S. Kim and D. T. Quang, *Chem. Rev.*, 2007, **107**, 3780; (d) D. M. Homden and C. Redshaw, *Chem. Rev.*, 2008, **108**, 5086; (e) G. Aragay, J. Pons and A. Merkoçi, *Chem. Rev.*, 2011, **111**, 3433; (f) Z. Xu, J. Yoon and D. R. Spring, *Chem. Soc. Rev.*, 2010, **39**, 1996; (g) P. A. Gale and R. Quesada, *Coord. Chem. Rev.*, 2006, **250**, 3219.
- 8 (a) S. Kolusheva, R. Zadmand, T. Schrader and R. Jelinek, *J. Am. Chem. Soc.*, 2006, **128**, 13592; (b) M. D. Lankshear, A. R. Cowley and P. D. Beer, *Chem. Commun.*, 2006, 612; (c) K.-C. Chang, I.-H. Su, G.-H. Lee and W.-S. Chung, *Tetrahedron Lett.*, 2007, **48**, 7274; (d) P. C. Riffaud, I. V. Duncker, A.-L. Marty, C. Richard, A. Prigent, F. Moati, L. S. Mantel, D. Scherman, M. Bessodes and N. Mignet, *Bioconjugate Chem.*, 2010, **21**, 589.
- 9 (a) J. S. Kim, S. Y. Lee, J. Yoon and J. Vicens, *Chem. Commun.*, 2009, 4791; (b) K.-C. Chang, I.-H. Su, Y.-Y. Wang and W.-S. Chung, *Eur. J. Org. Chem.*, 2010, 4700; (c) Z. Xu, J. Yoon and D. R. Spring, *Chem. Soc. Rev.*, 2010, **39**, 1996; (d) M. Kumar, R. Kumar and V. Bhalla, *Org. Lett.*, 2011, **13**, 366; (e) X. He and W. W. Yam, *Org. Lett.*, 2011, **13**, 2172; (f) X.-L. Ni, S. Wang, X. Zeng, Z. Tao and T. Yamato, *Org. Lett.*, 2011, **13**, 552; (g) J. McGinley and J. M. D. Walsh, *Inorg. Chem. Commun.*, 2011, **14**, 1018; (h) O. Sahin and M. Yilmaz, *Tetrahedron*, 2011, **67**, 3501.
- 10 (a) G. Yu, B. Hua and C. Han, *Org. Lett.*, 2014, **16**, 2486; (b) H. Zhang, X. Ma, K. T. Nguyen and Y. Zha, *ACS Nano*, 2013, **7**, 7853; (c) M. Xue, Y. Yang, X. Chi, Z. Zhang and F. Huang, *Acc. Chem. Res.*, 2012, **45**, 1294; (d) C. Li, X. Shu, J. Li, J. Fan, Z. Chen, L. Weng and X. Jia, *Org. Lett.*, 2012, **14**, 4126.
- 11 (a) L. Xu, M.-L. He, H.-B. Yang and X. Qian, *Dalton Trans.*, 2013, **42**, 8218; (b) X. Peng, J. Du, J. Fan, J. Wang, Y. Wu, J. Zhao, S. Sun and T. Xu, *J. Am. Chem. Soc.*, 2007, **129**, 1500; (c) T. Cheng, Y. Xu, S. Zhang, W. Zhu, X. Qian and L. Duan, *J. Am. Chem. Soc.*, 2008, **130**, 16160; (d) M. Taki, M. Desaki, A. Ojida, S. Iyoshi, T. Hirayama, I. Hamachi and Y. Yamamoto, *J. Am. Chem. Soc.*, 2008, **130**, 12564; (e) X. L. Tang, X. H. Peng, W. Dou, J. Mao, J. R. Zheng, W. W. Qin, W. S. Liu, J. Chang and X. J. Yao, *Org. Lett.*, 2008, **10**, 3653; (f) L. Xue, C. Liu and H. Jiang, *Org. Lett.*, 2009, **11**, 1655.
- 12 B. B. Shi, Y. M. Zhang, T. B. Wei, P. Zhang, Q. Lin and H. Yao, *New J. Chem.*, 2013, **37**, 3737.
- 13 R. K. Pathak, A. G. Dikundwar, T. N. Guru Row and C. P. Rao, *Chem. Commun.*, 2010, **46**, 4345.
- 14 (a) R. Joseph, J. P. Chinta and C. P. Rao, *Inorg. Chem.*, 2011, **50**, 7050; (b) R. K. Pathak, V. K. Hinge, A. Rai, D. Panda and C. P. Rao, *Inorg. Chem.*, 2012, **51**, 4994.
- 15 (a) J. Zhao, B. Zhao, J. Liu, A. Ren and J. Feng, *Chem. Lett.*, 2000, 268; (b) L. Wang, W. Qin, X. Tang, W. Dou and W. Liu, *J. Phys. Chem. A*, 2011, **115**, 1609; (c) H. Gorner, S. Khanra, T. Weyhermuller and P. Chaudhari, *J. Phys. Chem. A*, 2006, **110**, 2587; (d) J. Wu, W. Liu, J. Ge, H. Zhang and P. Wang, *Chem. Soc. Rev.*, 2011, **40**, 3483.
- 16 (a) R. J. Wandell, A. H. Younes and L. Zhu, *New J. Chem.*, 2010, **34**, 2176; (b) A. S. Al-Kady, M. Gaber, M. M. Hussein and E.-Z. Ebeid, *J. Phys. Chem. A*, 2009, **113**, 9474.
- 17 (a) L. Wang, W. Qin, X. Tang, W. Dou and W. Liu, *J. Phys. Chem. A*, 2011, **115**, 1609; (b) J. Wu, W. Liu, J. Ge, H. Zhang and P. Wang, *Chem. Soc. Rev.*, 2011, **40**, 3483.
- 18 (a) SAINT, Bruker-AXS, Madison, WI, 2010; (b) G. M. Sheldrick, *SADABS*, University of Gottingen, Germany, 2008; (c) G. M. Sheldrick, *Acta Crystallogr., Sect. A: Fundam. Crystallogr.*, 2008, **64**, 112; (d) A. L. Spek, *PLATON, A Multipurpose Crystallographic Tool*, Utrecht University, Utrecht, The Netherlands, 2010.
- 19 M. Thompson, *ArgusLab 4.0.1*, Planaria software LLC, Seattle, Wash, USA, 2004.

Copyright of Dalton Transactions: An International Journal of Inorganic Chemistry is the property of Royal Society of Chemistry and its content may not be copied or emailed to multiple sites or posted to a listserv without the copyright holder's express written permission. However, users may print, download, or email articles for individual use.